8-13-2016

(Magneto)caloric refrigeration: is there light at the end of the tunnel?

Vitalij K. Pecharsky
Iowa State University and Ames Laboratory, vitkp@ameslab.gov

Jun Cui
Iowa State University, cuijun@iastate.edu

Duane D. Johnson
Iowa State University, ddj@iastate.edu

(Magneto)caloric refrigeration: is there light at the end of the tunnel?

Abstract
Caloric cooling and heat pumping rely on reversible thermal effects triggered in solids by magnetic, electric or stress fields. In the recent past, there have been several successful demonstrations of using first-order phase transition materials in laboratory cooling devices based on both the giant magnetocaloric and elastocaloric effects. All such materials exhibit non-equilibrium behaviours when driven through phase transformations by corresponding fields. Common wisdom is that non-equilibrium states should be avoided; yet, as we show using a model material exhibiting a giant magnetocaloric effect, non-equilibrium phase-separated states offer a unique opportunity to achieve uncommonly large caloric effects by very small perturbations of the driving field(s).

Keywords
magnetocaloric effect, electrocaloric effect, elastocaloric effect, caloric materials, caloric cooling, caloric heat pumping

Disciplines
Energy Systems | Heat Transfer, Combustion | Materials Science and Engineering

Comments
This is a manuscripts of an article published as Pecharsky, Vitalij K., Jun Cui, and Duane D. Johnson. "(Magneto) caloric refrigeration: is there light at the end of the tunnel?." Phil. Trans. R. Soc. A 374, no. 2074 (2016): 20150305. DOI: 10.1098/rsta.2015.0305. Posted with permission.

Journal: **PHILOSOPHICAL TRANSACTIONS OF THE ROYAL SOCIETY A**

Article id: **RSTA20150305**

Article Title: **(Magneto)caloric refrigeration: is there light at the end of the tunnel?**

First Author: Vitalij K. Pecharsky

Corr. Author(s): Vitalij K. Pecharsky

AUTHOR QUERIES – TO BE ANSWERED BY THE CORRESPONDING AUTHOR

As the publishing schedule is strict, please note that this might be the only stage at which you are able to thoroughly review your paper.
Please pay special attention to author names, affiliations and contact details, and figures, tables and their captions.
No changes can be made after publication.

The following queries have arisen during the typesetting of your manuscript. Please answer these queries by marking the required corrections at the appropriate point in the text.

Q1	Reference [12] (in the author file) has been repeated and hence the repeated version has been deleted and then re-numbered. Please check.
Q2	While the online version of figure 2 will be in colour, we have been instructed to print the figure in black and white. Please note that if you have explicitly referred to colour in the caption this may affect the legibility of the figure in print.
Q3	We have changed the variable '$\mathbf{J}$' to 'J' here and elsewhere. Please check and confirm whether our change made is appropriate.

PHILOSOPHICAL TRANSACTIONS A

rsta.royalsocietypublishing.org

(Magneto)caloric refrigeration: is there light at the end of the tunnel?

Vitalij K. Pecharsky, Jun Cui and Duane D. Johnson

Ames Laboratory and the Department of Materials Science and Engineering, Iowa State University, Ames, IA 50011-3020, USA

VKP, 0000-0001-9503-7567

Review

Cite this article: Pecharsky VK, Cui J, Johnson DD. 2016 (Magneto)caloric refrigeration: is there light at the end of the tunnel? *Phil. Trans. R. Soc. A* 20150305. http://dx.doi.org/10.1098/rsta.2015.0305

Accepted: 5 May 2016

One contribution of 16 to a discussion meeting issue 'Taking the temperature of phase transitions in cool materials'.

Subject Areas:
energy, materials science

Keywords:
magnetocaloric effect, electrocaloric effect, elastocaloric effect, caloric materials, caloric cooling, caloric heat pumping

Author for correspondence:
Vitalij K. Pecharsky
e-mail: vitkp@ameslab.gov

Caloric cooling and heat pumping rely on reversible thermal effects triggered in solids by magnetic, electric or stress fields. In the recent past, there have been several successful demonstrations of using first-order phase transition materials in laboratory cooling devices based on both the giant magnetocaloric and elastocaloric effects. All such materials exhibit non-equilibrium behaviours when driven through phase transformations by corresponding fields. Common wisdom is that non-equilibrium states should be avoided; yet, as we show using a model material exhibiting a giant magnetocaloric effect, non-equilibrium phase-separated states offer a unique opportunity to achieve uncommonly large caloric effects by very small perturbations of the driving field(s).

This article is part of the themed issue 'Taking the temperature of phase transitions in cool materials'.

1. Introduction

Reversible thermal events in solids, aka *caloric* effects (the name 'caloric' derives from Latin *calor*, literally 'heat'), have been known for over a century—they occur when a constant 'control' field acting upon a material is perturbed. *Magneto*caloric, *electro*caloric and *elasto*caloric effects are all observed as materials' temperature (entropy) changes when the strength of *magnetic*, *electrical* or *stress* field, respectively, is altered adiabatically (isothermally). Underlying any and all caloric effects are specific components of the total entropy of a solid that can be most easily influenced by the perturbation of the corresponding control, or 'driving' field. Take a magnetic metal as an example, where three fundamental contributions to the total entropy can be recognized [1]: electronic (S_E), lattice (S_L) and magnetic (S_m). The magnetic entropy, which represents disorder of the

THE ROYAL SOCIETY PUBLISHING

individual magnetic moments, either electronic (spin and orbital) or nuclear or both, is most probably to be affected when the strength of a magnetic field surrounding the material is changed. As the magnetic field rises (falls) isothermally by $\pm\Delta H$, magnetic disorder generally gets reduced (increased), thus bringing the magnetic part of the total entropy down (up) by $\pm\Delta S_{\mathrm{m}}$. When ΔH is applied adiabatically, the total entropy ($S_{\mathrm{E}} + S_{\mathrm{L}} + S_{\mathrm{m}}$) of a solid must remain constant, hence as one component of the total entropy goes up (down) others must equivalently fall (rise) so that in our example $\Delta S_{\mathrm{E}} + \Delta S_{\mathrm{L}} + \Delta S_{\mathrm{m}} = 0$ as the result of the perturbation and, therefore, temperature of a solid must go down (up).

In the absence of losses, caloric effects can be exceptionally efficient forms of energy conversion. For example, magnetic moment–magnetic field coupling, being a quantum mechanical effect, approaches 100% efficiency when hysteresis and eddy currents are both negligible. The potential for producing reversible caloric effects with high efficiency in solids underpins a variety of cooling and/or heat pumping applications based on the magnetocaloric, elastocaloric and electrocaloric effects. Among the three, cooling using magnetocaloric effect is most mature. Following pioneering work by Debye & Giauque [2–4] in 1920s, adiabatic demagnetization refrigeration has become a well-established commercial technology routinely employed today to reach ultra-low temperatures in research environment. Some 50 years later, seminal work by Brown, Steyert and Barclay [5–9] demonstrated that magnetocaloric effect may be useful around room temperature, thus delineating a roadmap toward temperature spans much larger than the magnetocaloric effect itself, even if with zero cooling power at the time. Major breakthroughs occurred about 20 years later, when Pecharsky & Gschneidner [10–12] reported the discovery of the giant magnetocaloric effect in $Gd_5Si_2Ge_2$ and related compounds, and Zimm *et al.* [13] demonstrated a near-room-temperature magnetic refrigerator reliably producing cooling powers exceeding 500 W using elemental Gd while employing a 5 T driving field. These two developments opened a new chapter in magnetocaloric cooling, taking first steps toward the projected transformation of a laboratory curiosity into a line of commercial cooling devices using magnetocaloric effect [14].

Similar to magnetocaloric cooling, the feasibility of exploiting the electrocaloric effect has been demonstrated first at cryogenic temperatures by Radebaugh *et al.* [15,16], and later near-room temperature in several laboratory-scale devices by Sinyavsky & Brodyansky [17], Jia & Ju [18], Gu *et al.* [19,20] and Wang *et al.* [21]. Finally, elastocaloric cooling is getting some serious attention after Cui *et al.* [22,23] demonstrated a cooling device based on the principle suggested by Annaorazov *et al.* [24]. Despite a number of successful demonstrations, all three near-room temperature caloric cooling technologies remain in their infancy, mostly due to the facts that (i) caloric effects that can be produced in readily available driving fields without damaging a material are relatively weak; (ii) active regeneration is required to achieve the temperature span of a typical vapour-compression device and (iii) caloric material - caloric cooling/heat pumping device integration is, therefore, far from trivial.

Over the last 20 or so years various aspects of caloric materials and caloric refrigeration/heat pumping devices have been reviewed in a number of publications [25–41] and a few books [42,43]. Readers interested in details and the then-current state of the art are referred to all of these quality publications. As suggested by the title of this work, here we restrict ourselves to discussing materials-related issues that may lead to stronger caloric effects generated by driving fields that are easily produced and maintained, with the goal to support accelerated development of better caloric materials and, therefore, broad adoption of these solid-state caloric cooling technologies in the foreseeable future. Magnetocaloric materials will predominantly be employed as examples; however, most of the discussion below is expected to be applicable to all three categories of caloric solids.

2. Caloric effects: where are the limitations?

Rephrasing the key message from the last paragraph of the introduction, availability of materials with substantially enhanced caloric effects, achieved preferably in driving fields much reduced compared with those that are customary today is expected to both brighten the light at the end of the tunnel and considerably shorten the road through it. The first question we, therefore, must address is: Where are we today with respect to the fundamental limits of the three kinds of caloric effects of interest?

With gas constant R, total angular (spin) momentum J for 4f (3d) metals, molar magnetic entropy of a solid in which x is the molar fraction of identical magnetic moment-carrying species, the total available magnetic entropy, S_m, is limited to Q3

$$S_m = xR\ln(2J+1)\,\mathrm{J\,mol^{-1}\,K^{-1}}. \tag{2.1}$$

For purely magnetic phenomena, neglecting the electronic (C_E) and magnetic (C_m) specific heats, and assuming that the lattice molar specific heat, C_L, is at its limit of $3R\,\mathrm{J\,mol^{-1}\,K^{-1}}$ (the latter is a reasonable approximation around 300 K for many intermetallic compounds and metallic alloys), the fundamental limits for the *conventional magnetocaloric effect* are, therefore, easily established

$$\Delta S_m = \pm S_m \tag{2.2}$$

and

$$\Delta T_{ad} \cong \pm\left(\frac{x}{3}\right) T\,\ln(2J+1), \tag{2.3}$$

where ΔS_m is the isothermal magnetic entropy change, ΔT_{ad} is the adiabatic temperature change and T is the absolute temperature. Hence, for elemental Gd ($J=7/2$) at approximately 300 K, ΔS_m is limited to about $\pm17.3\,\mathrm{J\,mol^{-1}\,K^{-1}}$ ($\pm110\,\mathrm{J\,kg^{-1}\,K^{-1}}$ or $\pm0.87\,\mathrm{J\,cm^{-3}\,K^{-1}}$) and ΔT_{ad} is limited to about ±208 K. For a hypothetical M_2X compound (M is 3d element and X is non-magnetic) with the Curie temperature, T_C near 300 K, maximum ΔS_m and ΔT_{ad} are reduced to $\pm9.9\,\mathrm{J\,mol^{-1}\,K^{-1}}$ ($\pm3.9\,\mathrm{J\,mol^{-1}\,K^{-1}}$) and ±120 K (±46 K), respectively, when $J=5/2$ ($J=1/2$). These simple estimates are in agreement with more rigorous calculations of Tishin [44]. In reality, S_m is removed over a large range of temperatures, i.e. equation (2.2) is transformed into

$$|\Delta S_m| \ll |\pm S_m|, \tag{2.2a}$$

and magnetocaloric effect peaks near T_C, being proportional to $(\partial M/\partial T)\mathrm{d}H$ (M is magnetization, H is magnetic field). The fields required to reach the fundamental limits of ΔS_m and ΔT_{ad} exceed 10 000 kOe [44] and are, therefore, impractical. Readily available magnetic fields are always severely limited, and typically observed ΔT_{ad} are about 1–4 K for magnetic field change of about 10–15 kOe [28]—a minuscule fraction of the nature-imposed limits.

Most-studied magnetocaloric materials order magnetically via second-order phase transitions. A handful of them [27–29,39] exhibit magnetoelastic first-order phase transitions where the magnetic ordering/disordering may be coupled with either simple volume discontinuities or substantial rearrangements of the crystal lattices [10,45–48]. This coupling leads to the *giant magnetocaloric effect*, where the conventional magnetic moment-only part given by equations (2.1)–(2.3) may become strongly enhanced by an elastic contribution, which is the difference of the entropies of the low- and high-field polymorphs of the material, ΔS_{el} [48,49]. Obviously, the enhancement can only be expected when both ΔS_{el} and ΔS_m have identical signs because the total observed magnetic field-induced entropy change is $\Delta S_M = \Delta S_m + \Delta S_{el}$. Although we note that the separation of magnetic and elastic contributions is only formal because they are inseparable during a first-order magnetostructural phase transition—ΔS_m scales with ΔH [5,50], but ΔS_{el} necessarily becomes magnetic field-independent when ΔH exceeds a certain critical value that is sufficient to complete the rearrangement in the crystal lattice [48,51]. The difference in behaviour of these two thermodynamic quantities with field, taken together with the difference in behaviours of the conventional and giant magnetocaloric effects [52] allows for each to be quantified from the analysis of behaviour of the magnetocaloric effect as a function of ΔH [51,53,54]. Especially in low magnetic fields, ΔS_{el} may substantially exceed ΔS_m, which identifies a promising path forward toward magnetocaloric materials exhibiting very strong magnetocaloric effects in relatively weak magnetic fields.

Electrocaloric effect originates from the entropy changes associated with the variation in dipole order in a polar dielectric induced by an electric field. Switching between non-polar and polar phases isothermally (adiabatically) produces an entropy (temperature) change, $\pm\Delta S_d$ ($\pm\Delta T_{ad}$). The maximum dipolar entropy, S_d, in a polar dielectric is [55,56]

$$S_d = xR\ln(\Omega)\,\mathrm{J\,mol^{-1}\,K^{-1}}, \tag{2.4}$$

where Ω is the number of discrete equilibrium orientations of identical dipolar entities, and x is the same as in equation (2.1) but with respect to electric dipoles. Given that the difference between the conventional magnetocaloric and *conventional electrocaloric effects* lies in the nature of the ordering species (magnetic moments versus electric dipoles), both effects have comparable upper bounds [55], i.e.

$$\Delta T_{ad} \cong \pm\left(\frac{x}{3}\right) T\ln(\Omega). \tag{2.5}$$

When the electrocaloric effect is purely from dipolar ordering, ΔS_d and ΔT_{ad} are related to polarization, P, as

$$\left.\begin{aligned} \Delta S_d &\cong \pm\frac{1}{2}\beta P^2 \\ \text{and}\qquad \Delta T_{ad} &\cong \frac{\pm 1/2T\beta P^2}{C}, \end{aligned}\right\} \tag{2.6}$$

where $\beta = \ln(\Omega)/(\varepsilon_0\Theta)$, C is specific heat, ε_0 is vacuum permittivity and Θ is an effective Curie coefficient [55,57]. Hence, to realize a large electrocaloric effect, there must be a large $|\Delta S_d|$ associated with the change of P, and a dielectric material must support a large $|\Delta P|$ induced by an external field. Ferroelectrics (FEs) just above an FE (dipole-ordered)–paraelectric (PE, dipole-disordered) phase transition are most useful because of the largest electric field-induced $|\Delta P|$. Several ferroelectrics exhibit ΔT_{ad} in excess of 10 K and $|\Delta S_d|$ over $50\,\mathrm{J\,kg^{-1}\,K^{-1}}$ [58–60] near FE transitions, even if in fields approaching dielectric breakdown. We note that while it is easy to generate very strong electric fields in small gaps, generation of magnetic fields in excess of approximately 2 T generally requires superconducting magnets or bulky Halbach-like arrays [61]. Like magnetocaloric, the electrocaloric effect may be strongly enhanced by ΔS_{el}, i.e. become *giant electrocaloric effect* due to accompanying structural changes that result from ferroelastic coupling.

Elastocaloric (aka thermoelastic) effect is related to reversible crystallographic phase transformations [62,63]. The latter are central to the enhancement of spin- (dipole)-order effects in materials with giant magnetocaloric (electrocaloric) effects. In a way, elastocaloric refrigeration is similar to vapour-cycle cooling: both use stress to induce a phase transformation and use the corresponding entropy change, but the refrigerant is liquid/vapour for vapour cycle, and solid/solid for elastocaloric cooling [22].

For example, when a thermoelastic shape memory material under stress switches between austenitic and martensitic phases releasing or absorbing latent heat, $\Delta Q_{el} = \pm T\Delta S_{el}$, the entropy change can be experimentally determined from either direct calorimetric measurements [64] or indirectly from the Clausius–Clapeyron equation (p is pressure and ΔV is phase volume change):

$$\left.\begin{aligned} \Delta S_{el} &= \left(\frac{\partial p}{\partial T}\right)\Delta V \\ \text{and}\qquad \Delta T_{ad} &\cong \frac{-T\Delta S_{el}}{C_L}, \end{aligned}\right\} \tag{2.7}$$

assuming C_L remains nearly constant. Notably, simple thermodynamics-derived relationships similar to equations (2.1) and (2.4) are not applicable within the realm of elastocaloric materials, and density functional theory calculations of the electronic and phonon contributions to the total entropy based on the chemistry of a given material, as well as actual structures of both the austenitic and martensitic phases, are needed for *ab initio* predictions of ΔS_{el}.

For some NiTi-based alloys, $\Delta Q_{el} \cong 20\,\mathrm{J\,g^{-1}}$ [65] has been reported, giving $\Delta T_{ad} \cong 85\,\mathrm{K}$, assuming $C_L \cong 3R$. The maximum observed ΔT_{ad} is $\sim \pm 20\,\mathrm{K}$ [22], i.e. elastocaloric effect reaches approximately 25% of the maximum given by equation (2.7), yet this relatively high value has been achieved at tensile stress approaching stress at failure. Compared with magnetocaloric and electrocaloric effects, elastocaloric effect remains least explored for its applicability to caloric effect-based refrigeration and heat pumping applications.

To sum up, present day caloric materials realize only small fractions of their magnetic-to-thermal, electric-to-thermal or stress-to-thermal energy conversion potentials. Fields that are easy to produce, maintain and perturb, and certain not to damage a caloric material, are only resulting in caloric effects that are in the range of a few per cent of the corresponding limiting values. This is indeed quite encouraging for both basic and applied science of caloric materials and caloric-based devices as all of the known and, predictably, hitherto undiscovered systems and compounds are very far away from the respective performance plateaus, offering challenging yet truly exciting materials development opportunities with a high probability to achieve quite remarkable improvements in the future.

3. Non-equilibrium states: are they the light?

In addition to exhibiting best in each class caloric performance, first-order phase transitions are notorious for the occurrence of non-equilibrium states manifested as history dependence, kinetically arrested states, hysteresis and phase separation. These features are usually considered detrimental to caloric performance and have been routinely dealt with by adjusting chemistry to shift a promising system toward equilibrium behaviour, which often results in the suppression or even complete destruction of the first-order nature of the phase transition and, therefore, leads to much reduced, conventional caloric effects making thus modified materials rather common [12,66]. On the other hand, non-equilibrium phenomena are unique because of the potential for far greater changes of nearly all materials' properties, including caloric effects.

Consider a hypothetical caloric material system in the vicinity of a first-order phase transition. Two-dimensional phase diagrams drawn in driving field (Φ)–temperature (T) coordinates are schematically illustrated in figure 1. The diagram in figure 1*a* only shows the phase transition for the case when Φ increases at constant temperature, henceforth the 'direct' transformation. The 'reverse' phase transition when Φ changes in the opposite directions at $T = \text{const.}$ generally occurs in a different region of the diagram as shown infigure 1*b* because of hysteresis. The reverse transformation generally also involves phase separation. We note that Φ_{start} and Φ_{finish} correspond, respectively, to the finish and the start, T_{finish} and T_{start}, of the magnetostructural phase transitions when temperature varies at constant field.

Assume that the blue (dark grey) phase is ferromagnetic (FM) and that the pink (light grey) phase is paramagnetic (PM). We further assume that the driving magnetic *field is perturbed adiabatically*. When the magnetic field is increased from nearly zero by a small increment, $+\Delta\Phi$ (which is the shortest distance between point A or point C and the line indicating the maximum available field), the system moves along the slightly nonlinear paths $A \rightarrow B$ or $C \rightarrow D$ shown in figure 1*a* as nearly vertical arrows that reflect proportionality of the magnetocaloric effect to $\Phi^{2/3}$ [50]. The value of the exponent (2/3) derived from the mean field theory [50] is applicable to materials exhibiting conventional magnetocaloric effect. Small changes in the magnetization lead to small ΔS_m. A positive field increment reduces S_m ($\Delta S_m < 0$) and increases the temperature of the system. The resulting ΔT_{ad} is also proportional to $\Delta\Phi$ and because the latter is small, ΔT_{ad} is expected to be measurable but small as indicated by short horizontal arrows pointing at B and D. The system remains in the equilibrium state at the beginning and end of the field increment. When the field is then reduced adiabatically by $-\Delta\Phi$, the system returns, respectively, to either the point A or C following the reverse paths $B \rightarrow A$ or $D \rightarrow C$; here, $\Delta S_m > 0$ and $\Delta T_{ad} < 0$, both are identical in magnitude to the corresponding magnetic entropy and temperature changes when $\Delta\Phi > 0$, but with opposite signs. In the absence of energy losses, repeated cycling along either of the two described pathways will continue to very efficiently produce identical $\pm\Delta T_{ad}$ that are, unfortunately, weak.

A much different response is expected when the same magnetic field increment $+\Delta\Phi$ is applied when the system is initially in point E and moves along the path $E \rightarrow F$ illustrated

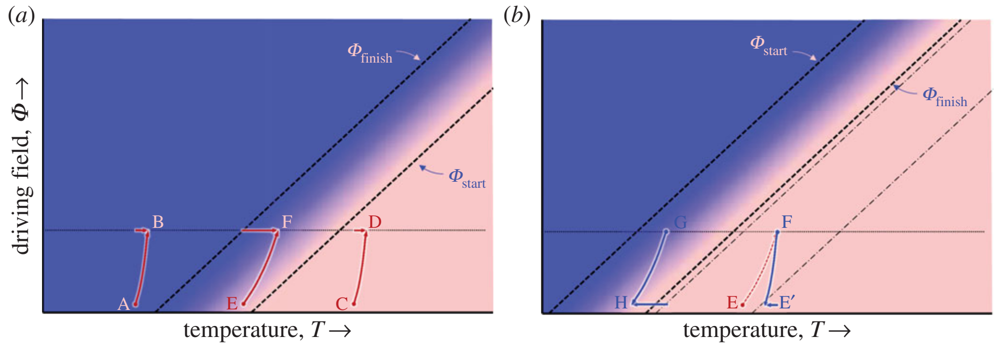

Figure 1. Schematic phase diagrams of a material exhibiting phase separation during the direct transformation shown in temperature (*T*)—driving field (Φ) coordinates when Φ increases (*a*), and during the reverse transformation when Φ is decreasing (*b*) at constant T. Solid colours represent single phase, equilibrium regions. The regions shown in gradient colour delineated with dashed lines represent non-equilibrium phase-separated states, where the dashed lines represent the start and finish of the direct (*a*) and reverse (*b*) phase transitions. In (*b*), the direct phase transition region delineated by the dashed-dotted lines is schematically shown for reference only without highlighting the phase separation. The horizontal dotted lines indicate the maximum available driving field. (Online version in colour.)

in figure 1*a*. Large changes in the relative concentrations of the coexisting phases scale nearly linearly with field and can be determined using the lever rule: e.g. x_1 is the volume fraction of PM phase and $1 - x_1$ for FM phase at point E and x_2 for PM and $1 - x_2$ for FM at point F. When added to the conventional $\Phi^{2/3}$ contribution, this leads to disproportionally large change in magnetization and S_m as the system moves from being predominantly paramagnetic ($x_1 > x_2$ in E) to predominantly ferromagnetic ($x_1 < x_2$ in F) and, therefore, a large ΔT_{ad}, as shown by the horizontal arrow pointing at point F will follow. Note that at the beginning (point E), the system is inside the non-equilibrium phase-separated state, and the value of x_1 will depend on the history, i.e. how the system has reached point E. Dependent on the actual magnitude of $\Delta\Phi$ the system may remain inside the non-equilibrium phase-separated state at the end (see figure 1*a*, point F), although it may also move into the equilibrium ferromagnetic state if the field increment is sufficiently large to cross the Φ_{finish} boundary. In either case, reducing the field by $-\Delta\Phi$ will *not* return the system to point E because of hysteresis.

Figure 1*b* illustrates the same region of temperatures and fields as figure 1*a*, except it now details the reverse phase transition which occurs when either or both temperature and field are reduced. The reverse phase transition also involves a non-equilibrium, phase-separated state; however, due to hysteresis, it is shifted to the left compared with figure 1*a*. The region of the direct phase transformation is delineated with thin dashed-dotted lines and shown for reference. The original path E → F discussed in the previous paragraph is now illustrated by a thin dotted arrow and it is assumed to have already occurred. Hence, in point F, the system consists of $1 - x_2$ FM phase, and x_2 PM phase where, according to figure 1*a*, $x_2 < 0.5$. A simple adiabatic removal of the field will not change x_2 because the system is outside the reverse phase transformation region. Then, both the ferromagnetic and paramagnetic phases present in the system will exhibit conventional and small magnetocaloric effects, both being proportional to $\Phi^{2/3}$. In the proximity of the phase transition, magnetocaloric effects in the paramagnetic and ferromagnetic states are nearly identical [52] and, therefore, the result will be a weighted average of the two equilibrium paths (B → A and D → C in figure 1*a*), shown schematically in figure 1*b* as path F → E′ with ΔT_{ad} (also being the weighted average), which is illustrated as a short horizontal arrow pointing at E′.

To realize the giant magnetocaloric effect upon field reduction, the system must be first moved into the point G; then $-\Delta\Phi$ will reduce volume fraction of the PM phase from x_2 to x_1 and produce a large $|\Delta T_{ad}|$, once again shown as a horizontal arrow pointing to H (figure 1*b*). Similar to field reduction starting from point F discussed in the previous paragraph, the positive field increment

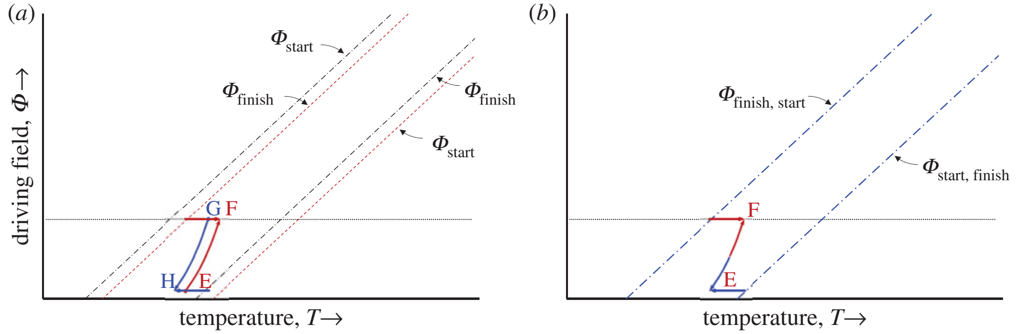

Figure 2. Schematic phase diagram illustrating two partially overlapping phase-separated regions (*a*). The direct phase transformation region is delineated with dashed (red) lines, and the reverse phase transformation region is delineated with dashed-dotted (blue) lines. Schematic phase diagram illustrating two completely overlapping phase-separated regions (*b*). The horizontal dotted lines indicate the maximum available driving field. (Online version in colour.) Q2

applied at point H will only lead to a small, conventional ΔT_{ad} (the weighted average of those shown in A → B and C → D) and, in order to induce the giant magnetocaloric effect again, the system must be shifted into point E before the next field application. The question is—*What, if any, can be done to move repeatedly along the* EFGH *loop and repeatedly trigger a giant magnetocaloric effect*?

One possible scenario is illustrated in figure 2*a*, where the hysteresis is much smaller compared with figure 1, and therefore, phase-separated states corresponding to the direct and reversed transformations largely, but not completely overlap. We note that reduction of hysteresis can be achieved without sacrificing the first-order nature of the phase transformation by engineering an appropriate microstructure that promotes both the direct and reverse transition; one example has been discussed by Moore *et al.* [67].

Assume that the system has reached the initial point E in exactly the same way as shown in figure 1*a*. For the positive $\Delta\Phi$ the system follows path E → F as already discussed above. Assuming that the volume fractions of the paramagnetic phase are, respectively, x_1 and x_2 in points E and F, and considering that point F is inside the reverse phase transformation region, a negative $\Delta\Phi$ will effectively move the system along the G → H line, however, not without an irreversible loss. Because the field-up and field-down half-cycles are fully contained within the corresponding phase-separated regions, the resulting ΔT_{ad} are expected to be nearly identical in magnitude but different in signs as illustrated by the matching horizontal arrows. Unfortunately, the irreversibility present in the complete EFGH cycle will result in a different x_1' at the point H compared with the initial state of the system in point F and after a few cycles the system will move into a steady, yet largely different, state with reduced magnetocaloric effect when compared with the 'virgin' EFGH cycle. This conclusion is in good agreement with direct cyclic ΔT_{ad} measurements reported for Heusler alloys, even though the measurements have been performed using $\Delta\Phi$ that were large enough to, at least initially, drive the material completely from the low-field into the high-field phase [68,69].

The desired location of phase fields is illustrated in figure 2*b*, where the phase-separated regions coincide for both the direct and reverse transformations. Clearly, the system can be cycled along the E → F and F → E paths indefinitely, triggering identical in magnitude and large ΔT_{ad}. Unfortunately, the situation depicted in figure 2*b* is difficult to realize for first-order phase transition materials in a restrictive planar system of coordinates implied by figures 1 and 2, that is, when only two thermodynamic variables (temperature and field) are available. The solution, which changes the playing field dramatically, is to add a third dimension (variable), for example, stress. Phases that coexist in the phase-separated region by definition must have different volumes. Similar to reduction of hysteresis observed when magnetizing/demagnetizing

Ni–Mn–In–Co at different hydrostatic pressures [70], applying (relieving) stress before driving the direct transformation by $+\Delta\Phi$ and relieving (applying) stress before initiating the reverse phase transition by $-\Delta\Phi$ can easily move the system from being characterized by different locations of the corresponding phase-separated regions in the T–Φ plane in figures 1 and 2*a* to the state depicted in figure 2*b*. Indeed, if stress (σ) is used to achieve the full coincidence of the direct and reverse phase-separated states, figure 2*b* is simply a projection of two planar cross sections of the three-dimensional phase diagram T–Φ–σ coordinates taken at fixed σ_1 and σ_2. Using stress requires additional energy, yet this is expected to be a small price to pay as it allows one to realize repeatedly very large $|\partial\Delta T_{\mathrm{ad}}/\partial\Delta\Phi|$.

4. Conclusion

There remains much to be learned about how to control the phase-separated states, and how to move efficiently a material along the paths that lead to repeatable caloric effects, even in the presence of hysteresis. Besides using extrinsic factors discussed here, i.e. by making use of a third dimension to solve an old two-dimensional hysteresis problem, there are numerous material design opportunities that remain worthy of exploration. The two most obvious possibilities include (i) incorporating both stress-inducing and stress-relieving microstructural features in a real material and (ii) designing real materials and transformation pathways without energy barriers. In the first, a specific set of microstructural features, such as stress-generating inclusions may seed and promote the transition from a high-volume to a low-volume phase, while stress-relieving voids may seed and promote the reverse, thus nearly closing the hysteresis gap. In the second, a promising path forward is establishing and reaching single-domain limits, where domains can switch without barriers, and seeking and following different pathways that are most energetically favourable individually for either the direct or reverse transformations. With this, we are ready to address the question that we asked in the title of this contribution: while there is more than one light at the end of the tunnel, non-equilibrium, phase-separated states are clearly one of the most important—promising to achieve a very large $|\partial\Delta T_{\mathrm{ad}}/\partial\Delta\Phi|$ in small applied fields, potentially leading to breakthroughs in design of caloric cooling and heat pumping devices.

Competing interests. We declare no competing interests.
Funding. This work is supported by the United States Department of Energy, Office of Science, Basic Energy Sciences Programs, Materials Sciences and Engineering Division. Ames Laboratory is operated by Iowa State University under contract no. DE-AC02-07CH11358 with the United States Department of Energy.

References

1. Gopal ESR. 1966 *Specific heat at low temperatures*. New York, NY: Plenum Press.
2. Debye P. 1926 Einige Bemerkungen zur Magnetisierung bei tiefer Temperatur. *Ann. Phys.* **81**, 1154–1160. (doi:10.1002/andp.19263862517)
3. Giauque WF. 1927 A thermodynamic treatment of certain magnetic effects. A proposed method of producing temperatures considerably below 1° absolute. *J. Am. Chem. Soc.* **49**, 1864–1870. (doi:10.1021/ja01407a003)
4. Giauque WF, MacDougall DP. 1933 Attainment of temperatures below 1 degrees absolute by demagnetization of $Gd_2(SO_4)_3 \cdot 8H_2O$. *Phys. Rev.* **43**, 768. (doi:10.1103/PhysRev.43.768)
5. Brown GV. 1976 Magnetic heat pumping near room temperature. *J. Appl. Phys.* **47**, 3673–3680. (doi:10.1063/1.323176)
6. Brown GV. 1978 Practical and efficient magnetic heat pump. *NASA Tech. Brief* **3**, 190–191.
7. Steyert WA. 1978 Stirling-cycle rotating magnetic refrigerators and heat engines for use near room temperature. *J. Appl. Phys.* **49**, 1216–1226. (doi:10.1063/1.325009)
8. Barclay JA, Steyert WA. 1982 Active magnetic regenerator. U.S. Patent No. 4,332,135.
9. Barclay JA. 1983 The theory of an active magnetic regenerative refrigerator. In *Proc. of the Second Biennial Conference on Refrigeration for Cryocooler Sensors and Electronic Systems, NASA-CP 2287*, p. 13. Greenbelt, MD: Goddrad Space Flight Center.

10. Pecharsky VK, Gschneidner Jr KA. 1997 Giant magnetocaloric effect in $Gd_5Si_2Ge_2$. *Phys. Rev. Lett.* **78**, 4494–4497. (doi:10.1103/PhysRevLett.78.4494)
11. Pecharsky VK, Gschneidner Jr KA. 1997 Tuneable magnetic regenerator alloys with a giant magnetocaloric effect for magnetic refrigeration from ∼20 to ∼290 K. *Appl. Phys. Lett.* **70**, 3299–3301. (doi:10.1063/1.119206)
12. Pecharsky VK, Gschneidner Jr KA. 1997 Effect of alloying on the giant magnetocaloric effect of $Gd_5Si_2Ge_2$. *J. Magn. Magn. Mater.* **167**, L179–L194. (doi:10.1016/S0304-8853(96)00759-7) Q1
13. Zimm CB, Jastrab A, Sternberg A, Pecharsky V, Gschneidner K, Osborne M, Anderson I. 1998 Description of performance of a near-room temperature magnetic refrigerator. *Adv. Cryo. Eng.* **43**, 1759–1766. (doi:10.1007/978-1-4757-9047-4_222)
14. Holzhäuzer V, Kapp H. 2015 Premiere of cutting-edge cooling appliance at CES 2015 Joint news release by BASF, Astronautics Corporation of America, and Haier. See https://www.basf.com/en/company/news-and-media/news-releases/2015/01/p-15–100.html.
15. Radebaugh R, Lawless WN, Siegwarth JD, Morrow AJ. 1979 Feasibility of electrocaloric refrigeration for the 4–15 K temperature range. *Cryogenics* **19**, 187–208. (doi:10.1016/0011-2275(79)90019-5)
16. Radebaugh R, Lawless WN, Siegwarth JD, Morrow AJ. 1980 Electrocaloric refrigeration at cryogenic temperatures. *Ferroelectrics* **27**, 205–2118. (doi:10.1080/00150198008226100)
17. Sinyavsky YV, Brodyansky VM. 1992 Experimental testing of electrocaloric cooling with transparent ferroelectric ceramic as a working body. *Ferroelectrics* **131**, 321–325. (doi:10.1080/00150199208223433)
18. Jia YB, Ju YST. 2012 A solid-state refrigerator based on the electrocaloric effect. *Appl. Phys. Lett.* **100**, 242901. (doi:10.1063/1.4729038)
19. Gu HM, Qian XS, Li XY, Craven B, Zhu WY, Cheng AL, Yao SC, Zhang QM. 2013 A chip-scale electrocaloric effect based cooling device. *Appl. Phys. Lett.* **102**, 122904. (doi:10.1063/1.4799283)
20. Gu HM, Qian XS, Ye HJ, Zhang QM. 2014 An electrocaloric refrigerator without external regenerator. *Appl. Phys. Lett.* **105**, 162905. (doi:10.1063/1.4898812)
21. Wang YD, Smulin SJ, Sheridan MJ, Wang Q, Eldershaw C, Schwartz DE. 2015 A heat-switch-based electrocaloric cooler. *Appl. Phys. Lett.* **107**, 134103. (doi:10.1063/1.4932164)
22. Cui J, Wu YM, Muehlbauer J, Hwang YH, Radermacher R, Fackler S, Wuttig M, Takeuchi I. 2012 Demonstration of high efficiency elastocaloric cooling with large ΔT using NiTi wires. *Appl. Phys. Lett.* **101**, 073904. (doi:10.1063/1.4746257)
23. Cui J, Takeuchi I, Wuttig M, Wu YM, Radermacher R, Hwang YH, Muehlbauer JR. 2012 Thermoelastic cooling. U.S. Patent Application 20120273158, November 1.
24. Annaorazov MP, Nikitin SA, Tyurin AL, Akopyan SA, Myndyev RW. 2002 Cooling scheme based on the AF-F transition in Fe-Rh alloys induced by tensile stress. *Phys. Stat. Sol. (a)* **194**, 304–314. (doi:10.1002/1521-396X(200211)194:1<304::AID-PSSA304>3.0.CO;2-4)
25. Andreyenko AS, Belov KP, Nikitin SA, Tishin AM. 1989 Magnetocaloric effects in rare earth magnetic materials. *Usp. Fizichesk. Nauk* **158**, 553–579. (doi:10.3367/UFNr.0158.198908a.0553)
26. Pecharsky VK, Gschneidner Jr KA. 1999 Magnetocaloric effect and magnetic refrigeration. *J. Magn. Magn. Mater.* **200**, 44–56. (doi:10.1016/S0304-8853(99)00397-2)
27. Gschneidner Jr KA, Pecharsky VK. 2000 Magnetocaloric materials. *Annu. Rev. Mater. Sci.* **30**, 387–429. (doi:10.1146/annurev.matsci.30.1.387)
28. Gschneidner Jr KA, Pecharsky VK, Tsokol AO. 2005 Recent developments in magnetocaloric materials. *Rep. Progr. Phys.* **68**, 1479–1539. (doi:10.1088/0034-4885/68/6/R04)
29. Brück E. 2005 Developments in magnetocaloric refrigeration. *J. Phys. D Appl. Phys.* **38**, R381–R391. (doi:10.1088/0022-3727/38/23/R01)
30. Pecharsky VK, Gschneidner Jr KA. 2006 Advanced magnetocaloric materials: what does the future hold? *Int. J. Refrig.* **29**, 1239–1249. (doi:10.1016/j.ijrefrig.2006.03.020)
31. Phan MH, Yu SC. 2007 Review of the magnetocaloric effect in manganite materials. *J. Magn. Magn. Mater.* **308**, 325–340. (doi:10.1016/j.jmmm.2006.07.025)
32. Planes A, Mañosa L, Acet M. 2009 Magnetocaloric effect and its relation to shape-memory properties in ferromagnetic Heusler alloys. *J. Phys. Condens. Matter* **21**, 233201. (doi:10.1088/0953-8984/21/23/233201)
33. Shen BG, Sun JR, Hu FX, Zhang HW, Cheng ZH. 2009 Recent progress in exploring magnetocaloric materials. *Adv. Mater.* **21**, 4545–4564. (doi:10.1002/adma.200901072)

34. De Oliveira NA, von Ranke PJ. 2010 Theoretical aspects of the magnetocaloric effect. *Phys. Rep. Rev. Sec. Phys. Lett.* **489**, 89–159. (doi:10.1016/j.physrep.2009.12.006)
35. Scott JF. 2011 Electrocaloric materials. *Annu. Rev. Mater. Res.* **41**, 229–240. (doi:10.1146/annurev-matsci-062910-100341)
36. Franco V, Blasquez JS, Ingale B, Conde A. 2012 The magnetocaloric effect and magnetic refrigeration near room temperature: materials and models. *Annu. Rev. Mater. Res.* **42**, 305–342. (doi:10.1146/annurev-matsci-062910-100356)
37. Vallant M. 2012 Electrocaloric materials for future solid-state refrigeration technologies. *Progr. Mater. Sci.* **57**, 980–1009. (doi:10.1016/j.pmatsci.2012.02.001)
38. Smith A, Bahl CRH, Bjork R, Engelbrecht K, Nielsen KK, Pryds N. 2012 Materials challenges for high performance magnetocaloric refrigeration devices. *Adv. Energy Mater.* **2**, 1288–1318. (doi:10.1002/aenm.201200167)
39. Tishin AM, Spichkin YI. 2014 Recent progress in magnetocaloric effect: mechanisms and potential applications. *Int. J. Refrig.* **37**, 223–229. (doi:10.1016/j.irefrig.2013.09.012)
40. Ozbolt M, Kitanowski A, Tusek J, Poredos A. 2014 Electrocaloric refrigeration: thermodynamics, state of the art and future perspectives. *Int. J. Refig.* **40**, 174–188. (doi:10.1016/j.irefrig.2013.11.007)
41. Takeuchi I, Sandeman K. 2015 Solid-state cooling with caloric materials. *Phys. Today* **68**, 48–54. (doi:10.1063/PT.3.3022)
42. Tishin AM, Spichkin YI. 2003 *The magnetocaloric effect and its applications.* Bristol, UK: Institute of Physics Publishing.
43. Kitanowski A, Tusek J, Tome A, Plaznik U, Ozbolt M, Poredos A. 2015 *Magnetocaloric energy conversion. From theory to applications*. New York, NY: Springer.
44. Tishin AM. 1990 Magnetocaloric effect in strong magnetic fields. *Cryogenics* **30**, 127–136. (doi:10.1016/0011-2275(90)90258-E)
45. Morellon L, Algarabel PA, Ibarra MR, Blasco J, Garcia-Landa B. 1998 Magnetic-field-induced structural phase transition in $Gd_5(Si_{1.8}Ge_{2.2})$. *Phys. Rev. B* **58**, R14721–R14724. (doi:10.1103/PhysRevB.58.R14721)
46. Dung NH, Zhang L, Qu ZQ, Bruck E. 2011 From first-order magneto-elastic to magneto-structural transition in $(Mn,Fe)_{1.95}P_{0.5}Si_{0.5}$ compounds. *Appl. Phys. Lett.* **99**, 092511. (doi:10.1063/1.3634016)
47. Fujita A, Fujieda S, Fukamichi K, Mitamura H, Goto T. 2001 Itinerant-electron metamagnetic transition and large magnetovolume effects in La(FexSi1-x)13 compounds. *Phys. Rev. B* **65**, 014410. (doi:10.1103/PhysRevB.65.014410)
48. Pecharsky VK, Holm AP, Gschneidner Jr KA, Rink R. 2003 Massive magnetic-field-induced structural transformation in Gd_5Ge_4 and the nature of the giant magnetocaloric effect. *Phys. Rev. Lett.* **91**, 197204. (doi:10.1103/PhysRevLett.91.197204)
49. Tegus O, Brück E, Buschow KHJ, De Boer FR. 2002 Transition-metal-based magnetic refrigerants for room-temperature applications. *Nature* **415**, 150–152. (doi:10.1038/415150a)
50. Oesterreicher H, Parker FT. 1984 Magnetic cooling near Curie temperature above 300 K. *J. Appl. Phys.* **55**, 4334–4338. (doi:10.1063/1.333046)
51. Pecharsky VK, Gschneidner Jr KA. 2007 Magnetocaloric effect associated with magnetostructural transitions. In *Magnetism and structure in functional materials* (eds A Planes, L Manosa, A Saxena). Berlin, Germany: Springer.
52. Pecharsky VK, Gschneidner Jr KA, Pecharsky AO, Tishin AM. 2001 Thermodynamics of the magnetocaloric effect. *Phys. Rev. B* **64**, 144406. (doi:10.1103/PhysRevB.64.144406)
53. Chernyshov AS, Tsokol AO, Tishin AM, Gschneidner Jr KA, Pecharsky VK. 2005 Magnetic and magnetocaloric properties and the phase diagram of single crystal dysprosium. *Phys. Rev. B* **71**, 184410. (doi:10.1103/PhysRevB.71.184410)
54. Gschneidner KAJr, Mudryk Y, Pecharsky VK. 2012 On the nature of the magnetocaloric effect of the first-order magnetostructural transition. *Scr. Mater.* **67**, 572–577. (doi:10.1016/j.scriptamat.2011.12.042)
55. Pirc R, Kutnjak Z, Blinc R, Zhang QM. 2011 Upper bounds on the electrocaloric effect in polar solids. *Appl. Phys. Lett.* **98**, 021909. (doi:10.1063/1.3543628)
56. Pirc R, Kutnjak Z, Blinc R, Zhang QM. 2011 Electrocaloric effect in relaxor ferroelectrics. *J. Appl. Phys.* **110**, 074113. (doi:10.1063/1.3650906)

57. Lu SG, Zhang QM. 2009 Electrocaloric materials for solid state refrigeration. *Adv. Mater.* **21**, 1983–1987. (doi:10.1002/adma.200802902)
58. Mischenko AS, Zhang Q, Scott JF, Whatmore RW, Mathur ND. 2006 Giant electrocaloric effect in thin-film $PbZr_{0.95}Ti_{0.05}O_3$. *Science* **311**, 1270–1271. (doi:10.1126/science.1123811)
59. Neese B, Chu BJ, Lu SG, Wang Y, Furman E, Zhang QM. 2008 Large electrocaloric effect in ferroelectric polymers near room temperature. *Science* **321**, 821–823. (doi:10.1126/science.1159655)
60. Lu SG, Rožič B, Zhang QM, Kutnjak Z, Neese B. 2011 Enhanced electrocaloric effect in ferroelectric poly(vinylidene-fluoride/trifluoroethylene) 55/45 mol % copolymer at ferroelectric-paraelectric transition. *Appl. Phys. Lett.* **98**, 122906. (doi:10.1063/1.3569953)
61. Lee SJ, Kenkel JM, Pecharsky VK, Jiles DC. 2002 Permanent magnet array for the magnetic refrigerator. *J. Appl. Phys.* **91**, 8894–8896. (doi:10.1063/1.1451906)
62. Quarini J, Prince A. 2004 Solid state refrigeration: cooling and refrigeration using crystalline phase change in metal alloys. *Proc. Inst. Mech. Eng.* **218**, 1175–1178. (doi:10.1243/0954406042369062)
63. Bonnot F, Romero R, Mañosa L, Vives E, Planes A. 2008 Elastocaloric effect associated with the martensitic transition in shape-memory alloys. *Phys. Rev. Lett.* **100**, 125901. (doi:10.1103/PhysRevLett.100.125901)
64. Marcos J, Casanova F, Battle X, Labarta A, Planes A, Mañosa L. 2003 A high-sensitivity differential scanning calorimener with magnetic field for magnetostructural transitions. *Rev. Sci. Instrum.* **74**, 4768–4771. (doi:10.1063/1.1614857)
65. Shaw JA, Churchill CB, Iadicola MA. 2008 Tips and tricks for characterizing shape memory alloy wire: part 1—differential scanning calorimetry and basic phenomena. *Exp. Technol.* **32**, 55–62. (doi:10.1111/j.1747-1567.2008.00410.x)
66. Provenzano V, Shapiro AJ, Shull RD. 2004 Reduction of hysteresis losses in magnetic refrigerant $Gd_5Si_2Ge_2$ by the addition of iron. *Nature* **429**, 853–857. (doi:10.1038/nature02657)
67. Moore JD, Morrison K, Perkins GK, Schlagel DL, Lograsso TA, Gschneidner Jr KA, Pecharsky VK, Cohen LF. 2009 Metamagnetism seeded by nanostructural features of single-crystalline $Gd_5Si_2Ge_2$. *Adv. Mater.* **21**, 3780–3783. (doi:10.1002/adma.200900093)
68. Titov I, Acet M, Farle M, Gonzalez-Alonso D, Manosa L, Planes A, Krenke T. 2012 Hysteresis effects in the inverse magnetocaloric effect in martensitic Ni-Mn-In and Ni-Mn-Sn. *J. Appl. Phys.* **112**, 073914. (doi:10.1063/1.4757425)
69. Gottschall T, Skokov KP, Frincu B, Gutfleisch O. 2015 Large reversible magnetocaloric effect in Ni-Mn-In-Co. *Appl. Phys. Lett.* **106**, 021901. (doi:10.1063/1.4905371)
70. Liu J, Gottschall T, Skokov KP, Moore JD, Gutfleisch O. 2012 Giant magnetocaloric effect driven by structural transitions. *Nat. Mater.* **11**, 620–626. (doi:10.1038/NMAT3334)